JOURNAL OF MATERIALS SCIENCE **34** (2000) 3441–3446

Compression testing of pultruded carbon fibre-epoxy cylindrical rods

C. SOUTIS
Department of Aeronautics, Imperial College of Science, Technology and Medicine, Prince Consort Road, London, SW7 2BY, UK
E-mail: c.soutis@ic.ac.uk

The fibre waviness inherent in conventional prepreg laminates significantly reduces their compressive strength. This waviness can be reduced through the use of unidirectional fibre rods. In this work, the development of a new test procedure and specimen design is reported that was used to determine the compressive properties of pultruded T300/828 and IM7/828 carbon fibre-epoxy unidirectional rods at room temperature. The IM7/828 system demonstrates a higher compressive strength than the T300/828 composite due to stronger fibres used and fewer manufacturing defects. Since the fibres as in tension primarily carry the compressive load, the final fracture of the rods occurs when the fibres fail. Post-failure examination reveals that failure of the fibres is microbuckling-induced. This is a bending failure as a consequence of buckling. Other events such as fibre-matrix debonding (splitting) and matrix yielding do not by themselves cause the final failure, but they facilitate fibre buckling by reducing the lateral support for the fibres. Microbuckling failure models are used to predict the compressive strength of the carbon fibre rods; agreement between theory and experiment is acceptable.

1. Introduction

Fibre waviness within a conventional laminate severely degrades the compressive strength and stiffness of composites [1, 2]. Prepreg tape has an inherent waviness, which is compounded during subsequent layering and compaction. Automated tow placement reduces waviness during placement but does not eliminate it during compaction and cure. Recently, aircraft manufacturers and fibre suppliers recognised the potential benefits of minimising fibre waviness by producing small diameter unidirectional carbon fibre rods that could lead to the design of more efficient laminate structures, especially under compressive loading.

The measurement of the compressive response of carbon fibre reinforced plastics (CFRP) has always presented difficulties. This is because compression testing is sensitive to factors such as Euler buckling, specimen misalignment in the test fixture, fibre misalignment in the specimen and bending/stretching coupling in the laminate. Therefore, special care is required in the specimen design and test procedure.

Over the years, various test methods have been developed to measure longitudinal compressive strength of unidirectional flat plates [3–5] but there is no universally acceptable test procedure for cylindrical rods loaded in compression. The aim of the present investigation is to study the compressive behaviour of unidirectional carbon fibre-epoxy rods. A new test method and specimen design is developed. Foil type strain gauges bonded to the specimen with standard strain gauge adhesives are used to monitor the rod's stress-strain response. Optical microscopy is employed to assess material quality and scanning electron micrographs are examined to identify unique fracture characteristics. Strength results are compared to theoretical predictions obtained from several analytical fibre microbuckling failure models.

2. Experimental procedure

2.1. Materials

Unidirectional pultruded cylindrical rods of commercially available T300 and IM7 carbon fibres ($\approx$0.67 fibre volume ratio) in Epon 828 epoxy resin were tested; the rods were supplied by Cookson plc, UK. The pultrusion process generally consists of pulling continuous rovings through a resin bath and then into pre-forming fixtures where the section is partially shaped and excess resin and/or air are removed. Then it passes through a heated die (120°C–180°C), which consolidates and forms the shape, and cures the system. Suitable positioning and tensioning of the reinforcement is required so that it is presented to the die accurately and consistently. Fibre waviness is detrimental in compression, because it initiates fibre microbuckling resulting in premature failure of the composite.

2.2. Specimen geometry and test method

Thirty test specimens in total were cut from the unidirectional composite rods using a diamond-tipped saw. They have an almost circular cross-section and the

diameter was about 1.7 mm for the IM7/828 and 4 mm for the T300/828 rods; diameter variation is less than 2%. The overall specimen length is 33 mm and the gauge length is 13 mm, designed to avoid Euler buckling. The specimens were instrumented with 1 mm long strain gauges on either side of the gauge section to measure strain and any bending. The specimens were end-loaded in a modified Monsanto (Hounsfield) tensometer of 20 kN load capacity, compressed at a rate of 1 mm/min. Load and strain data were continuously recorded by an IBM-based data logging system.

Successful testing of end-loaded coupons depends upon the fibres terminating exactly at the interface on the end to ensure uniform loading. It is very difficult to achieve uniform contact between the end faces of the specimen and the surfaces of the platens of the testing machine. On loading premature failure of the specimen may occur before the entire end face of the coupon comes into contact with the platen. Usually, the specimen starts to split in the region near the loaded edge of its end face, and the crack tends to propagate along the length of the specimen causing premature failure. To avoid this, special steel end caps were manufactured and bonded to the specimens, Fig. 1. Specimen ends were then polished in a jig to ensure that they were flat and normal to the loading axis. The steel caps serve a double purpose in that they reduce end failures in the CFRP and provide adequate restraint against geometric buckling of the specimen.

Several specimens were cross-sectioned and observed under the optical microscope in order to assess their quality (voids content, resin rich regions and fibre waviness). Also, segments of tested rods containing the fracture surface of interest were cut, cemented to aluminium mounts and examined in an International Scientific Instruments ISI-DS 130 dual stage scanning electron microscope (SEM) to identify failure modes.

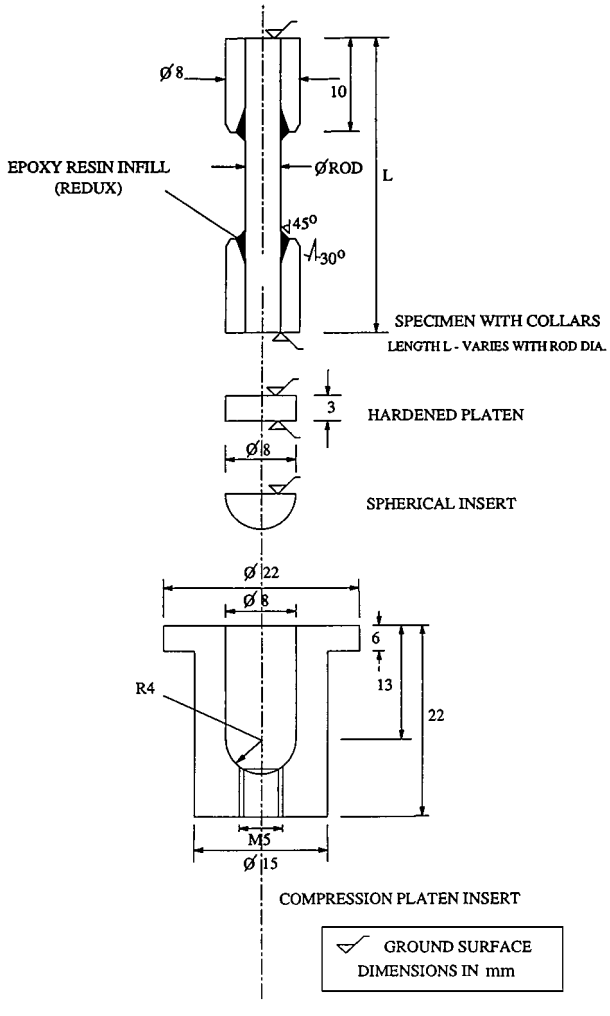

Figure 1 Specimen configuration and compression platen insert.

3. Test results and discussion

3.1. Fibre volume and weight fractions

One of the most important factors determining the mechanical properties of composites is the relative proportion of the matrix (resin) and reinforcing materials (fibres). The relative proportions can be given as the weight fractions or the volume fractions. From resin burn off tests it was found that the fibre volume fraction (V_f) for the T300/828 and IM7/828 was approximately 0.665, which is close to the value quoted by the material manufacturer (0.67). Alternatively, the weight fraction of the carbon fibres could be determined by chemical digestion of the resin.

The fibre volume fraction can be obtained from the following expression

$$V_f = \frac{\rho_{ce}}{\rho_f} w_f \tag{1}$$

where ρ_{ce} = composite density (i.e., mass/volume), ρ = fibre density and w_f = fibre weight fraction. It was found: $\rho_{ce}^{T300} = 1559$ kg/m^3 and $\rho_{ce}^{IM7} = 1612$ kg/m^3. The density values and other material properties for the fibres and the resin are presented in Table I.

3.2. Voids and resin rich regions

The presence of voids in the composite reduces its strength and elastic modulus since they reduce the volume of solid, within which the stresses are distributed. Also, voids can act as sites of local stress concentration that can initiate failure. Higher void contents usually mean lower fatigue resistance, greater susceptibility to water penetration and weathering, and increased variation in mechanical properties. The compressive strength is affected most, because the fibres have less side support by the resin and buckle at lower applied loads. The knowledge of void content is desirable for estimation of the quality of the composite. A good composite should have less than 1% voids, whereas a poorly manufactured composite can have up to 5% void content.

TABLE I Material properties (Manufacturer's data)

Property	T300	IM7	Epon 828
Tensile strength, MPa	3650	5313	92
Modulus, GPa	231	301	3.04
Failure strain, %	1.4	1.81	6.10
Density, kg/m^3	1760	1780	1220
Fibre diameter, μm	7	5	-

The volume fraction of voids can be calculated from the following expression

$$V_v = \frac{\rho_{ct} - \rho_{ce}}{\rho_{ct}} \quad (2)$$

ρ_{ct} is the theoretical composite density obtained from the rule of mixtures, i.e.

$$\rho_{ct} = V_f \rho_f + (1 - V_f)\rho_m \quad (3)$$

where ρ_m is the matrix density. Substituting the material properties of Table I in Equations 2 and 3 we get a void content of less than 1%. However, in Equation 3 ρ_m is assumed to be the same in the composite as it is in an unreinforced bulk state. Although it is necessary to use this assumption in our calculations, it may not be correct. Differences in heat and pressure during the cure cycle, and interaction with the reinforcement surface may affect the *in situ* resin density. It is thought that the bulk density is lower, making the void content seem lower than it really is. Assuming a 10% increase in the *in situ* resin density, Equation 2 predicts a void content of more than 3%, which is in better agreement with optical microscopy observations.

Fig. 2a shows the polished cross section of a selected T300/828 rod, revealing the existence of voids (10–12 μm in length and width) and resin rich regions. It also reveals different types of cross sectional fibre shapes, circular, elliptical and 'kidney' shaped; the 'kidney' shaped cross section fibres exhibited the highest density and were uniformly distributed within the composite. It can also be seen that in some locations the fibres are in contact with each other. This is not desirable because cracks are passing from one fibre to another causing premature failure of the composite. Fibre bunching was observed to occur more readily towards the centre of the rod rather than around its circumference. This type of fibre distribution in the T300/828 rod is typical of other specimens tested in the current study. Similar manufacturing defects were observed in the IM7/828 composite but considerably less than the case of the 4 mm rod and with more circular fibres, Fig. 2b.

Fibre imperfections, resin rich regions and voids affect the mechanical behaviour of the composite considerably. Under uniaxial compression they can initiate fibre microbuckling and cause premature failure of the composite. In order to get more accurate measurements of V_v and model the effect of defects (resin rich regions, cracks, etc.) on the compressive strength, further work is required.

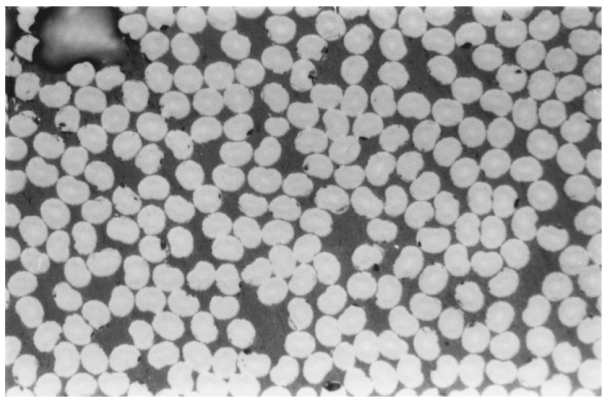

Figure 2a Cross section of a selected T300/828 rod showing voids and resin rich regions. The fibres ($d_f \approx 7\,\mu$m) of mainly 'kidney' shape are randomly distributed and in some locations are in contact with each other.

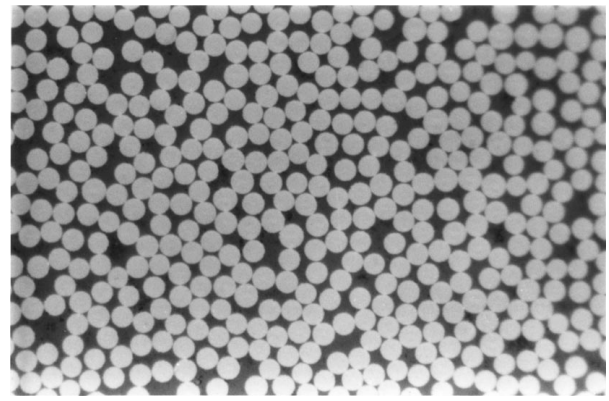

Figure 2b Cross section of a selected IM7/828 composite rod ($d_f \approx 5\,\mu$m). Manufacturing defects can be seen but are considerably less than those observed in the T300/828 rods.

3.3. Fibre waviness

In pultruded composite rods, fibre waviness may occur due to unsuitable positioning and non uniform tensioning of the reinforcement before it enters the heated die. This can cause a dramatic reduction in the compressive strength/stiffness properties of the composite. A theoretical study [6] has shown that a misalignment angle between the fibres and the loading axis of only 0.25° is sufficient to reduce the compressive strength of the XAS/914 carbon-epoxy system from 2720 MPa to 1800 MPa (i.e., more than 40% reduction). At 3° this is reduced to 700 MPa. The actual compressive strength of the XAS/914 system is generally considered to be about 1400 MPa [6]. However, values ranging from 885 MPa to 1990 MPa have been reported [7]. These differences are attributed to different testing methods used but also due to fibre misalignment effects.

Optical micrographs of T300/828 and IM7/828 rod specimens revealed a fibre misalignment between 1°–3° from the loading axis that increases significantly from the edge towards the centre of the rod. Also, broken fibres, resin rich regions and cracks running parallel to the fibre length have been observed. The crack widths are approximately 10–20 μm and are attributed to thermal stresses generated during processing, due to the differences in thermal coefficients of expansion of the resin and fibres when cured.

3.4. Compressive stress-strain data

The strength/stiffness properties of a composite material depend strongly on the properties of its constituents (resin, fibres) and their distribution and physical and chemical interactions. They also depend on the fabrication process and testing method. Defects introduced during manufacturing, like voids, resin rich regions, fibre misalignment and fibre breakage, reduce the compressive strength/stiffness dramatically. The currently examined cylindrical rods (T300, IM7/828) have been

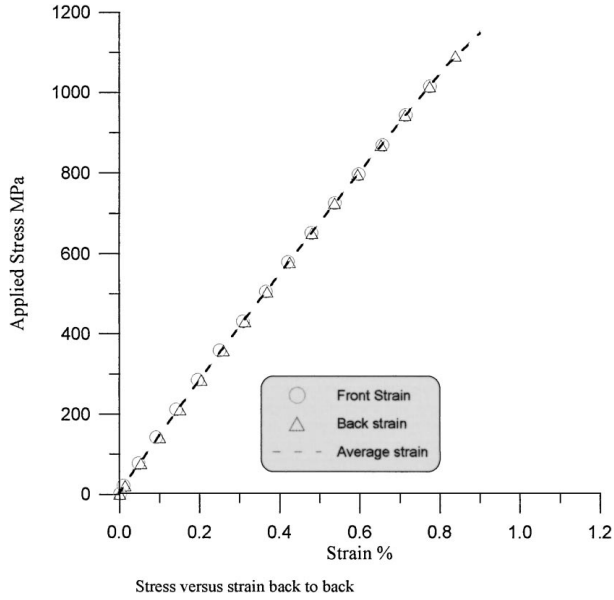

Figure 3 Typical compressive stress-strain response of a T300/828 rod.

produced by pultrusion and many of the defects described above have occurred during production. Their compressive strength is less than 50% of the theoretically predicted (rule of mixtures) tensile strength ($\sigma_T \approx V_f\sigma_f$).

The room temperature stress-strain response of a selected T300/828 specimen is shown in Fig. 3. The longitudinal strain on the two faces of the coupon is almost the same indicating negligible bending. Bending cannot be totally avoided in compression testing. It may be the result of initial imperfections in the specimen. The elastic modulus in the loading direction, measured at 0.25% strain is about 139 GPa, the failure strength is 1175 MPa and the mean failure strain 0.9%. The IM7/828 rods break in a similar brittle manner but showed higher strength/stiffness properties than the T300/828 due to better material quality (smaller rod diameter) and stronger fibres. The failure stress is 1676 MPa, the failure strain is 1.182% and the secant Young's modulus at 0.25% strain is 180 GPa. Compressive strength results of all specimens tested are summarised in Table II.

Note that the results quoted in Table II are based on the average of fifteen specimens tested for each composite system at room temperature level; the coefficient of variation is about 7.4% for the T300/828 and less than 5% for the IM7/828 composite. When the grip failures are not included in the calculations, the average compressive strength of the T300/828 rod is 1187 (±65) MPa and for the IM7/828 is 1648 (±25) MPa. However, grip failures do occur and therefore it will be quite appropriate in any design exercise to use the strength data presented in Table II.

TABLE II Compressive strength properties of unidirectional rods

Composite system	Average failure strength /MPa	Average failure strain %	Stiffness E_c/GPa
T300/828	1136 (±84)	0.929 (±0.063)	131 (±7.5)
IM7/828	1568 (±75)	1.127 (±0.059)	186 (±5.9)

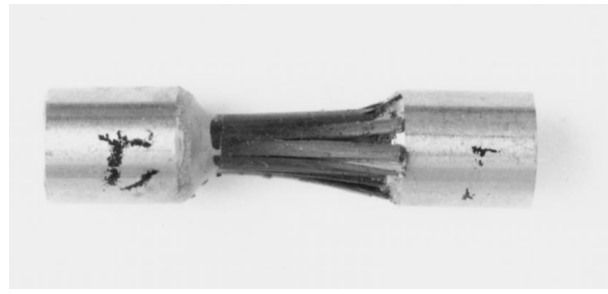

Figure 4 Overall compressive failure of a T300/828 composite rod.

3.5. Failure modes

Failure of both composite systems examined is sudden and catastrophic, giving a brush-like appearance, Fig. 4. Some grip failures still occur due to local stress concentrations in the end fittings. To avoid this completely specimens with waisted gauge section should be used [1]. The effect of waisting the gauge section is to cause failure in the central part of the specimen, but fibre damage and splitting may occur during the machining process. Grip failure is considered as premature failure of the specimen, which suggests that the results represent a lower bound on the strength.

The investigation of failure modes by fractographic methods is cumbersome because of the extensive post-failure damage. The release of strain energy from both the specimen and the test machine causes a substantial amount of fibre-matrix splitting, making it difficult to identify the main failure mode. However, careful examination of the broken specimens, suggests fibre microbuckling as the critical damage mechanism, which causes the catastrophic fracture. Longitudinal splits and fibre/matrix debonding do not occur gradually but take place suddenly and concurrently with the final failure. The SEM micrograph in Fig. 5 shows failure due to microbuckling. The fibres break at two points, which creates a band of about 8–10 fibre diameters long. The microbuckle can start from a pre-existing material defect, like wavy fibres, a void or resin rich region. Also, any weakening of the matrix or fibre/matrix interface occurring during manufacture increases the probability of buckling of the fibres, which results in degraded compressive strength.

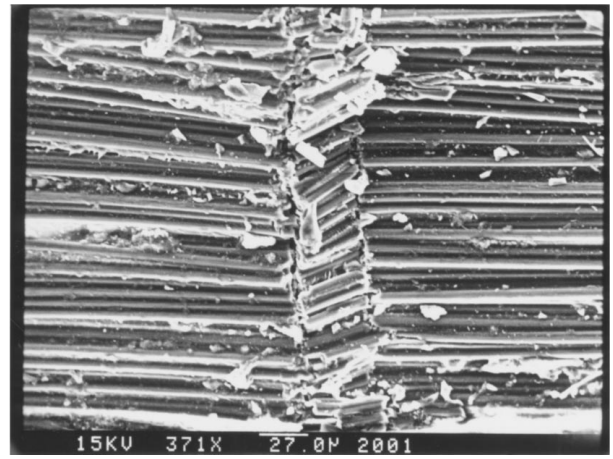

Figure 5 Fibre microbuckling failure mode observed in a T300/828 unidirectional rod.

4. Compressive strength prediction

The composite strength is not easily related to fibre and matrix properties since the compressive strengths of the constituents, especially of the fibres, are usually not known. Experimental results overwhelmingly support a linear relation between compressive strength and fibre volume fraction V_f (except for large values when $V_f > 0.8$) [8]. However, the Rosen model [9], gives an inverse relation between compressive strength and volume fraction, i.e.,

$$\sigma_c = \frac{G_m}{1 - V_f} \tag{4}$$

where G_m is the matrix shear modulus. For the current composite systems the compressive strength is an order of magnitude lower than that predicted by Equation 4.

It has been suggested that the composite fails at the matrix yield strain, ε_{my} [10]. Thus the compressive strength for the unidirectional rods in the fibre direction is given by

$$\sigma_c = (V_f E_f + V_m E_m)\varepsilon_{my} \tag{5}$$

where E's are the elastic moduli and the subscripts f and m refer to the fibre and matrix, respectively. Equation 5 suggests that the fibre compressive strength has no effect on the compressive strength of the composite and hence it can be applied to systems with strong fibres. It gives the required variation of strength with V_f and to fit the measured data for the T300/828 and IM7/828 composite rods, a matrix yield strain of about 0.8% has to be assumed. At present, the yield strain of the in situ resin is not known and further work is needed in order to investigate the validity of Equation 5.

Weaver and Williams [11] modelled the microbuckling process as a beam on an elastic foundation. The fibres bend at a critical strain and break, and the microbuckle then propagates across the width of the specimen by transfer of load to neighbouring fibres, which are already buckled by the axial strain. The critical composite stress is given by the Euler buckling formula as follows

$$\sigma_c = \left(\frac{\pi d_f}{4 w_k}\right)^2 E_c \tag{6}$$

where d_f is the fibre diameter, w_k is the kink-band length and E_c is the longitudinal stiffness of the composite. The model can make good strength predictions but requires experimental measurements of the w_k/d_f ratio. From the SEM micrograph, Fig. 5, it can be seen that the length of the microbuckled zone w_k is about 8 fibre diameters. Using this value in Equation 6 the predicted strength for the T300/828 is $\sigma_c^{T300} = 1262$ MPa and for the IM7/828 is $\sigma_c^{IM7} = 1802$ MPa. This is 10%–15% higher than the experimental strength results. Equation 6 shows that the compressive strength depends on fibre stiffness ($E_c \approx V_f E_f$) and diameter.

Argon [12] and Budiansky [13] have developed a theory of plastic microbuckling of unidirectional composites and give an expression for the critical buckling stress, σ_c, as

$$\sigma_c = \frac{\tau_y}{\phi} \tag{7}$$

where τ_y is the shear yield stress of the composite and ϕ is the fibre waviness. For the T300/828 and IM7/828 assuming $\tau_y = 60$ MPa and substituting in Equation 7 the measured compressive strengths we obtain $\phi = 3^\circ$ and 2°, respectively, which are similar to the values observed in the current sectioning studies. Budiansky and Fleck [14] have shown that variations in the shear yield stress ($\delta\tau_y$), elastic shear modulus (δG), and initial fibre misalignment ($\delta\phi$) are related to a change ($\delta\sigma_c$) in the critical stress by:

$$\frac{\delta\sigma_c}{\sigma_c} = \left(\frac{\sigma_c}{G}\right)\frac{\delta G}{G} + \left(1 - \frac{\sigma_c}{G}\right)\frac{\delta\tau_y}{\tau_y} - \left(1 - \frac{\sigma_c}{G}\right)\frac{\delta\phi}{\phi} \tag{8}$$

Thus, for instance, if $\sigma_c/G = 1/4$, a fractional increase of shear yield stress is three times as effective in raising the critical buckling stress as is a similar relative change in the shear modulus, and the same is true for a fractional decrease in the initial fibre imperfection. Fleck and co-workers [15–17] have considered the effect of combined remote axial compression and in-plane shear loading, random initial fibre waviness, and plastic strain hardening on the predicted critical stress for microbuckling. These models require knowledge of the shear strength properties, the initial fibre imperfection or the spectral density of fibre misalignment and the kink band orientation angle, β. Angle β is a post-failure geometric parameter, which depends on fibre imperfection (short-wave or long-wave), the elastic modulus of the laminate in the transverse direction, the shear modulus and the kinking failure stress, σ_c [18]. It is also difficult to explain precisely how σ_c will vary with fibre properties and content.

Steif [19, 20] has proposed a model to predict the remote compressive strain at which initially misaligned fibres break in tension as a result of bending. This model is an extension of Rosen's analysis [9] to situations in which matrix plasticity occurs and accounts for fibre bending stiffness and fibre volume fraction. It predicts the strength of practical composites successfully, but the geometry of the kink band needs to be known.

In more recent studies Berbinau and Soutis [21, 22] obtained a general microbuckling equation where a 0° fibre is modelled as an Euler slender column supported by a non-linear foundation (matrix):

$$E_f I \frac{d^4(v - v_0)}{dx^4} + \frac{A_f \sigma_0}{V_f}\frac{d^2 v}{dx^2} - A_f G(\gamma)\frac{d^2(v - v_0)}{dx^2} = 0 \tag{9}$$

where E_f is the fibre modulus, I is the second moment of inertia, A_f is the fibre cross section area, $v_0(x)$ is a sine function related to the initial fibre amplitude (waviness) and $G(\gamma)$ is the composite shear modulus that varies with the shear strain γ. Equation 9 is solved numerically using the MATHEMATICA [23] software and gives a relationship for the compressive stress σ_0 developed in the fibres in terms of the maximum amplitude v of the 0° buckled fibre during uniaxial compression.

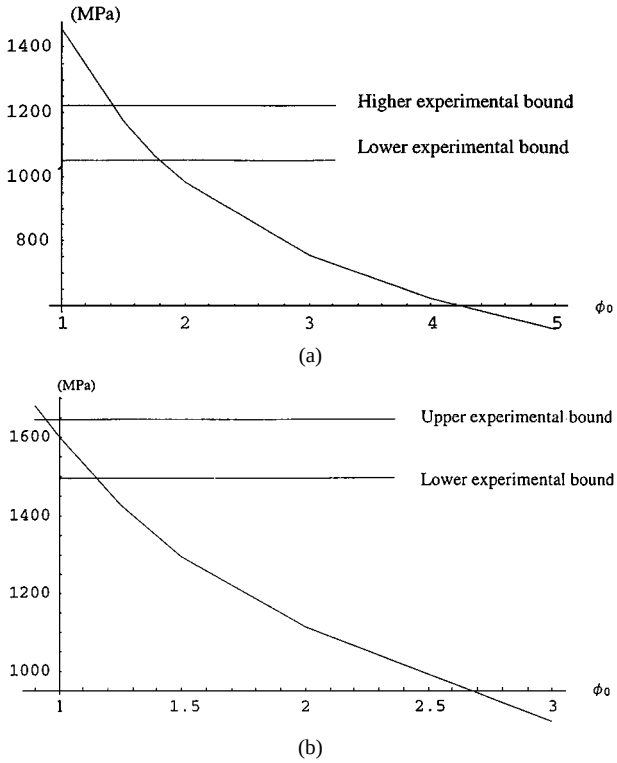

Figure 6 Compressive failure stress vs initial fibre misalignment. (a) for a unidirectional T300/828 rod and (b) IM7/828 rod.

Failure of the unidirectional material occurs when the fibre amplitude v starts to increase asymptotically. In Fig. 6 the compressive strength results for the two composite rods, T800/828 and IM7/828, are compared to theoretical predictions obtained from the Berbinau and Soutis fibre kinking model [22]. A good correlation is observed when the assumed initial fibre waviness ϕ is between 1° and 2°, which is similar to fibre misalignments revealed by optical microscopy (1°–3°).

5. Conclusions

At present, there is no standard compression test procedure to determine the compressive strength of pultruded composite rods. This work reports on the development of a novel test method and specimen design, which was used to measure the compressive properties of T300/828 and IM7/828 composite rods. The new test method overcomes the misalignment problem and is relatively easy to use. Most of the failures occur within the gauge length, but grip failures still happen due to the discontinuity in the end fittings. To avoid grip failures completely, specimens with waisted gauge section could be used, but there is always the danger of damaging the fibres. All existing compression test methods for flat specimens suffer from stress concentrations and produce reduced compressive strengths. Only a rigorous stress analysis will be able to quantify the loss in measured strength due to the induced stress concentration, but this is out of the scope of the present work.

The T300/828 and IM7/828 rods break in a brittle manner at approximately 1% strain due to fibre microbuckling. This is a fibre instability failure mode during which the fibres debond from the resin and break in bending. The strain at which this failure mode occurs is reduced with increasing void content, resin rich regions and fibre waviness. All these defects facilitate fibre buckling by reducing the side support for the fibres. The IM7/828 composite rods showed considerably fewer manufacturing defects and their compressive strength was 15%–20% higher than equivalent specimens made out of unidirectional prepreg tape. Suitable tensioning of the reinforcement during the pultrution process is crucial on eliminating fibre waviness and a further improvement in material quality by reducing voids could substantially increase the strength properties of the composite rods.

Existing theoretical models suggest that compressive strength is resin-dominated property, giving acceptable strength predictions, but further work is required to account explicitly for the effect of voidage, resin-rich regions and fibre-matrix interface on the compressive response; hygrothermal effects and long term behaviour need also to be considered.

Acknowledgements

The author would like to thank his research students for assisting with the collection of experimental data and Cookson plc for supplying the pultruded composite rods.

References

1. C. SOUTIS, *Composite Science and Technology* **42** (1991) 373.
2. *Idem.*, ASTM STP 1242, *American Society for Testing and Materials*, Philadelphia, PA, 1992, p. 168.
3. ASTM Standard D 3410-87, *American Society for Testing and Materials*, Philadelphia, PA, 1992.
4. K. E. HOFER, JR. and P. N. RAO, *Journal of Testing and Evaluation* **5**(4) (1977) p. 278.
5. M. J. SHUART, ASTM STP 734, *American Society for Testing and Materials*, 1981 p. 152.
6. M. R. WISNOM, *Composites* **21**(5) (1990) p. 403.
7. D. H. WOOLSTENCROFT, A. R. CURTIS and R. I. HARESCENGH, *ibid.* **12** (1981) p. 275.
8. M. R. PIGGOTT and P. WILDE, *J. Mater. Sci.* **15** (1980) p. 2811.
9. B. W. ROSEN, "Fibre composite materials" (*American Society of Metals*, 1965) p. 37.
10. T. HAYASHI and K. KOYAMA, in "Proceedings of the 5th International Conference on the Mechanical Behaviour of Materials" (Society of Materials Science, Kyoto, 1972) p. 104.
11. C. W. WEAVER and J. G. WILLIAMS, *J. Mater. Sci.* **10** (1975) p. 1323.
12. A. S. ARGON, "Treatise of Materials Science and Technology, Vol. 1" (Academic Press, New York, 1972).
13. B. BUDIANSKY, *Computers & Structures* **16**(1–4) (1983) p. 3.
14. B. BUDIANSKY and N. A. FLECK, *J. Mech. Phys. Solids* **41** (1993) p. 183.
15. W. S. SLAUGHTER, N. A. FLECK and B. BUDIANSKY, *J. Engng. Mats. and Technology* **115**(3) (1993) p. 308.
16. S. SIVASHANKER, N. A. FLECK and M. P. F. SUTCLIFFE, *Acta Mater*. **44**(7) (1996) p. 2581.
17. N. A. FLECK, S. SIVASHANKER and M. P. F. SUTCLIFFE, *Europ. J. Mech. & Solids* (special issue) **16** (1997) p. 65.
18. C. SOUTIS and D. TURKMEN, *Applied Composite Materials* **2**(6) (1995) p. 327.
19. P. S. STEIF, *Int. J. Solids & Structures* **16** (1990) p. 549.
20. *Idim., ibid.* **16** (1990) p. 563.
21. P. BERBINAU, C. SOUTIS and I. A. GUZ, *Composites Science & Technology* **59** (1999) p. 1451.
22. P. BERBINAU, C. SOUTIS, P. GOUTAS and P. T. CURTIS, *Composites: Part A* **30** (1999) p. 1197.
23. S. WOLFRAM, "MATHEMATICA" (Reading MA, Addison-Wesley, 1993).

Received 20 October 1999
and accepted 20 January 2000